Natural Hazards (2025) 121:2397–2417
https://doi.org/10.1007/s11069-024-06990-7

ORIGINAL PAPER

Improving the seismic resilience index of a school building

Zubair Sediqi[1] · **Ebru Harmandar**[1]

Received: 12 March 2024 / Accepted: 21 October 2024 / Published online: 12 November 2024

Abstract
The aim of the seismic resilience of a structural system is to prevent, minimize or decrease the damages (loss of life, social, economic, structural, and non-structural damages) that occur due to earthquakes. The seismic resilience of structures is one of the most interesting topics in the fields of earthquake and structural engineering. The meaning of the word 'resilience' differs from field to field, but in earthquake and structural engineering, resilience means keeping the functionality of a structural system after it has been damaged (Bruneau et al. 2003). A seismic resilience analysis of a school building in Milas, Mugla, a high-risk area in Turkey, is conducted. The current research focuses on examining pushover analysis, fragility curves, vulnerability curves, and functionality curves to evaluate the seismic resilience of the school building. The methodology for the assessment of the damage depends on HAZUS MH MR4 (2003), with the building modeled using SAP2000 software. Nonlinear pushover analysis is performed. Three different models are utilized to finally form the residence curve. It is examined the impact of these models on the resilience curves. The research is important in uncovering the effect of the models designed for utilization in the regional or building-based resilience analysis. Furthermore, it emphasizes the factors affecting the characteristics of the resilience curve. Consequently, this analysis aims to contribute to enhancing the attributes of the seismic resilience of school buildings or buildings with identical structural features.

Keywords Seismic resilience · School buildings · Damage assessment · Functionality of buildings · Recovery analysis

1 Introduction

One of the appealing subjects in earthquake engineering revolves around the seismic resilience of buildings and infrastructure. It has been a popular and one of the most discussed topics for researchers in earthquake engineering in recent years. The explanation of resilience varies across different fields. In the context of earthquake and structural engineering, resilience refers to the ability of a structural system to return to its functionality after

✉ Ebru Harmandar
ebruharmandar@mu.edu.tr

[1] Faculty of Engineering, Department of Civil Engineering, Muğla Sıtkı Koçman University, Muğla, Turkey

sustaining damage (Fig. 1). Moreover, seismic resilience holds consequence for economical purposes and the safety of individuals, particularly in regions prone to earthquakes. Assessing the seismic resilience of a structural system involves various evaluations, including damage assessment, determination of the design response spectrum, and the investigation of functionality curves through a structured procedure.

The mathematical formula derived for resilience (R) is (Bruneau et al. 2003):

$$\mathrm{R} = \int_{t1}^{t2} [100 - Q(t)]dt \tag{1}$$

where Q(t) is the functionality of a structural system as a function of time.

A resilient system, as defined by Bruneau et al. (2003), should have the following characteristics.

Robustness: the strength or capability of a structure to endure an event without losing the functionality of the structural system, particularly the undamaged components.

Redundancy: the availability of substitutional structural elements which replace those that are destroyed or lost their functionality due to earthquakes.

Resourcefulness: the ability to identify risky conditions that pose a threat to the structure, potentially causing damage to certain structural elements or systems.

Rapidity: the time in which the structure can regain its desired functionality following an event.

The seismic resilience was initially introduced by Bruneau et al. (2003). Subsequently, Bruneau and Reinhorn (2004) extended the concept to assess the resilience of critical care facilities, considering factors such as quality of life (total health population) and hospital capacity. Their study encompassed both structural and non-structural elements. Researchers have proposed to develop a suitable seismic resilience methodology for acute care facilities. Cimellaro et al. (2005) performed a framework for the resilience of hospitals, applying it to a Californian hospital. This methodology considered crucial resilience factors, including loss function (direct and indirect losses) and fragility curves for structural damage assessment. Cimellaro et al. (2010a) later enhanced the seismic resilience methodology for hospitals, including uncertainties such as losses, recovery time, intensity parameters, and response parameters. This methodology was applied to six hospitals in Memphis, USA, considering several rehabilitation strategies. The study concluded that the rebuild strategy showed the highest resilience and quality of function, albeit being the most uneconomical case.

The methodology to enhancing resilience differs between individual buildings and a collection of buildings within a specific region. In the case of regional structures, the

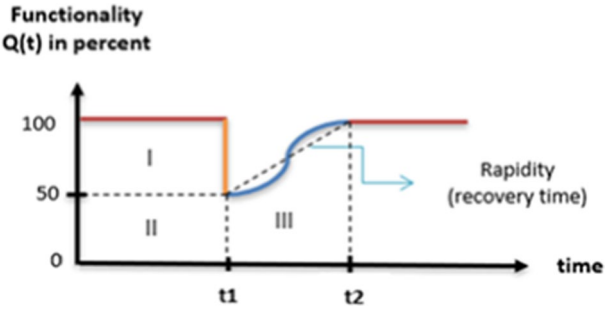

Fig. 1 Definition of seismic resilience of a structural system (Bruneau et al. 2003)

resilience methodology is applied based on categorizing building inventories according to various characteristics such as geometry and number of stories. Burton et al. (2017) proposed a resilience framework for regional buildings. This research outlines repairing strategies for each limit states (collapse, demolish, irreparable damages, loss of functionality) of a structure. Furthermore, a non-linear time history analysis is conducted to assess damage and develop fragility curves. Xiong et al. (2019) proposed a methodology for the seismic resilience of Beijing city. Non-linear time history analysis and the FEMA-P58 methodology are employed to generate fragility curves and evaluate the residual functionality of each building in the aftermath of earthquakes in the region. Similar to hospitals, schools are one of the most important civil engineering structures. Researchers and engineers have been exploring suitable and secure approaches to enhance the resilience of school buildings. In recent years, several studies have been focused on the resilience of school buildings. Samadian et al. (2019) performed a research study on a reinforced concrete (RC) school building, utilizing vulnerability curves. The authors concluded that resilience functionality obtained through vulnerability curves gives more accurate results than those derived from fragility curves. Motlagh et al. (2020) evaluated the seismic resilience of RC school buildings considering the effects of carbonate corrosion. The authors found that corrosion undesirably impacts the resilience of structures. González et al. (2020) performed a research study on the resilience of school buildings in Mexico using an event-based assessment methodology. They concluded that one-story buildings are more resilient than two-story buildings, as the latter experience higher casualties due to structural and non-structural damages. Finally, Sardari et al. (2020) analyzed a seismic resilience case study of a high school steel building. The proposed framework was applied to both retrofitted and un-retrofitted school building. The study showed that the loss of functionality in retrofitted buildings is decreased, contributing to increased resilience. In addition to buildings, numerous studies have been conducted on the seismic resilience of other civil engineering structures (e.g., bridges, electrical power systems etc.) using various methodologies and frameworks. For example, Zhao and Sun (2021) performed a research study representing how dynamic and looped interdependencies affect the resilience of a critical infrastructure systems. Seismic resilience principles can be applied across various engineering fields (e.g., hydraulic, electric etc.). For instance, Yoon et al. (2021) conducted a flow-based study on the resilience of water network transmission systems.

Furthermore, resilience analysis incorporates the functionality of a structure, evaluating decrease in its operational capabilities, and developing appropriate actions to restore its functionality. The focus is on determining how rapidly a building can gain its original functionality again following a severe event, such as an earthquake. Key considerations include post-event functionality, redundancy, and the building's capacity for rapid recovery after enduring a significant earthquake.

Additionally, strength analysis involves the assessment of a building's structural capacity under standard operating conditions. This analysis specifically examines a structure's ability to withstand both static forces, such as dead and live loads, and dynamic forces like wind, aiming to prevent structural failure under these conditions. Strength analysis is one of the steps taken to obtain resilience analysis.

Resilience is a developing concept within the field of earthquake engineering. Understanding the behavior of structures after a significant earthquake is crucial for executing post-earthquake precautions. In the future, the resilience analysis will play a crucial role in municipal operations and decision-making procedures. The operative status of public buildings, mainly hospitals and schools, becomes significantly important in the aftermath of an earthquake. This study focuses on applying the concept of resilience to assess the

seismic resilience of a school building. The primary objective is to demonstrate how various approaches to calculating the resilience index can influence the ultimate result.

This study examines the resilience of a high school building located in Milas/Mugla, Turkey. According to the General Directorate of Mineral Research and Exploration of Turkey (AFAD), Mugla is identified as a hazardous and earthquake-prone area with numerous active faults. The main fault zones in this region are Büyük-Menderes fault zone, Karaova-Milas fault zone, Muğla-Yatağan fault zone, Gökova fault zone, and Fethiye-Burdur fault zone. The predominant fault direction in this area is generally from east to west, characterized by lateral, strike-slip, and normal mechanisms (Ince and Yılmazoğlu 2021). Notably, the school building is situated in the Milas district, near the Karaova-Milas active fault zone. Consequently, conducting a thorough analysis of the resilience of this school becomes vital.

This study aims to contribute to the development of seismic resilience in school buildings, leading to potential reductions in social, economic damages, and fatalities. Furthermore, it pursues to assist engineers and civilians in preventing or minimizing casualties during earthquakes, improving the seismic resilience of school buildings, executing precautions for future seismic events, refining the design of school buildings in the region for post-earthquake scenarios, and evaluating the probability of building damage and loss of functionalities. The methodology of this study will cover critical topics, including design spectrum, modeling, building capacity, damage assessment (fragility and vulnerability curves), and functionality curves.

2 Methodology

The framework adopted for this study is presented in Fig. 2.

The first step toward this topic is determining the design response spectrum for the targeted region where the school building is located. For this purpose, the necessary data is obtained from the Disaster and Emergency Management Presidency (AFAD) of Turkey. In the second step, the school building is modeled using SAP2000 software, and a nonlinear static pushover analysis is performed to assess the seismic response of the structure. Once the pushover analysis is complete, a damage assessment is conducted, and fragility curves are generated for various damage levels (Slight, Moderate, Extreme, Collapse). Subsequently, vulnerability curves are derived from the combination of these fragility curves. In the final part of the study, the seismic resilience diagram of the structure is produced.

2.1 Performance analysis of a structure

2.1.1 Seismic capacity

For the analysis of the structures and consequently generating the capacity curve of the structure, it is required to achieve a nonlinear static pushover analysis of the building. In this study, the SAP2000 software is employed for modeling and analyzing the structure. The pushover analysis method, a widely used incremental monotonic static analysis approach, is utilized for evaluating the seismic performance of buildings. Therefore, this study focuses on analyzing the seismic performance of the structure through nonlinear static pushover analysis. The capacity curve (pushover curve) of a structure is derived by

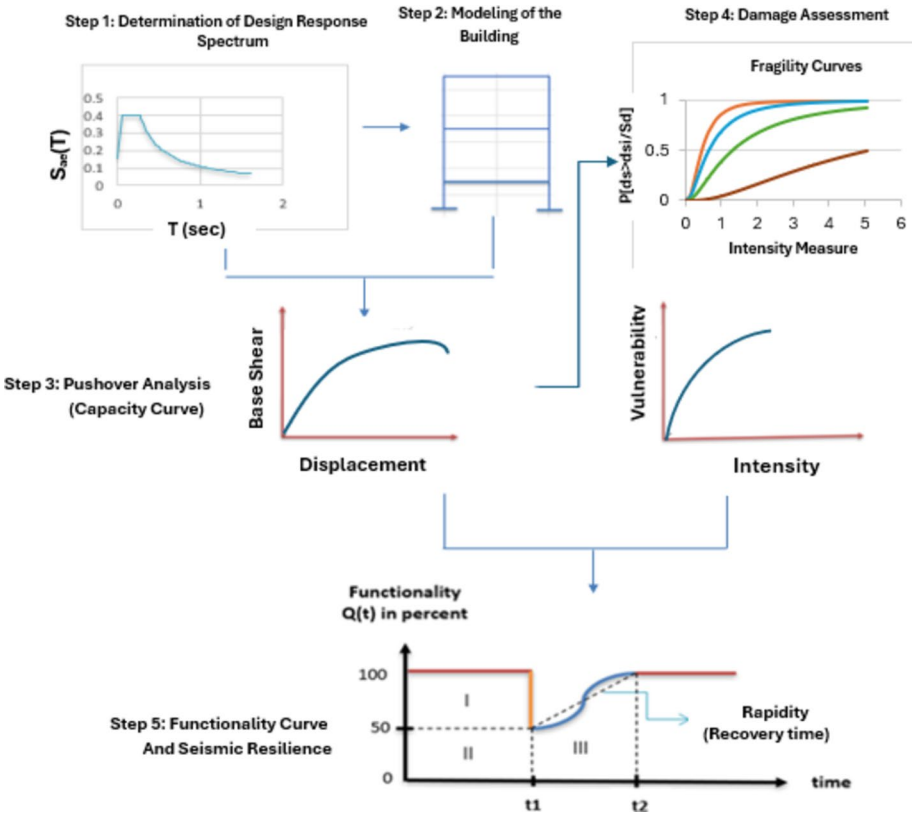

Fig. 2 Framework of the study (after Samadian et al. 2019)

considering roof displacement and base shear of the building under monotonic lateral loads and the self-weight (dead load) of the structure (Freeman et al. 1975).

A capacity curve consists of three control points (Fig. 3) known as *Design capacity, Yield capacity*, and *Ultimate capacity.* Design capacity exemplifies the nominal strength of a building, while yield capacity indicates the real strength of a building. The final

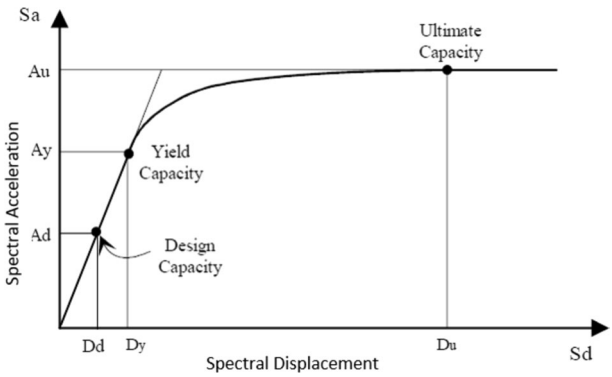

Fig. 3 Control points of a building capacity curve (HAZUS MH MR4, 2003)

control point signifies the maximum strength that a building can withstand. Hence, the structure loses its elasticity and reaches the plastic stage (HAZUS MH MR4, 2003).

2.1.2 Performance levels and seismic damage

In the analyses, another crucial issue involves assigning the plastic hinges to beams and columns. M3 and P-M2-M3 hinges are designated to both ends of the beam and columns, respectively, while the whole structure is assumed to be diaphragm in the vertical global direction (Z). The plastic hinges have several performance levels (plastic hinge deformations) as shown in Fig. 4. By referencing these plastic hinge deformations, we can estimate the potential damages that may occur in the structure.

The damage level gradually increases from point A to point C. At point C, the structure fails, loses its functionality suddenly, and as a result it will collapse. Each performance level is associated with a specific damage definition, as outlined by Hamadamin (2014):

(A-B) performance level: very small damages that can be ignored or require minimal repairs.

(B-IO) performance level: limited or very slight structural damages may occur, but the systems and building structure remain reasonably functional.

(IO-LS) performance level: due to structural and non-structural damages, a low life safety threat is expected.

(LS-CP) performance level: Possibility of collapse, with the building frame experiencing structural damage. Consequently, the structure may no longer withstand lateral forces and can only support gravity loads.

For a more comprehensive understanding, Fig. 5 shows detailed information on the damage and performance levels of a structure.

2.2 Damage assessment

Damage assessment of structures can be categorized into two main parts: Fragility analysis, Vulnerability analysis.

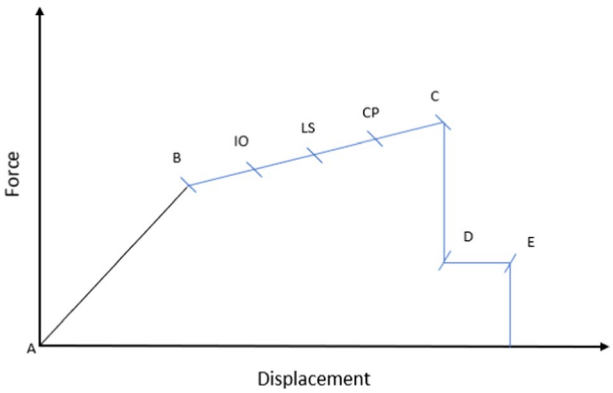

Fig. 4 Performance levels of plastic hinges (FEMA 356)

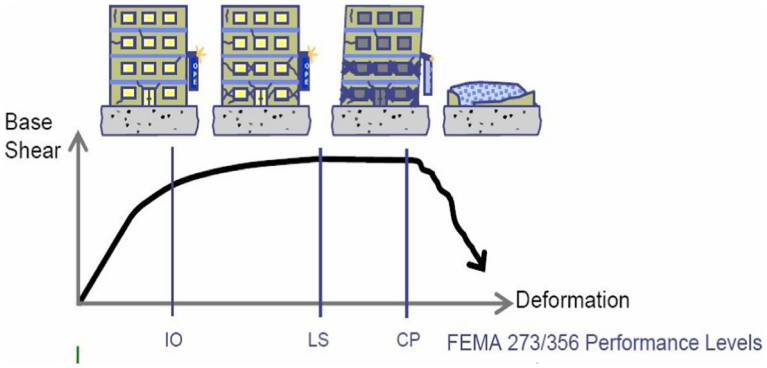

Fig. 5 Performance levels of a building (FEMA 273/356)

2.2.1 Fragility analysis

Fragility analysis, also named as fragility curves, is a widely used method for predicting loss estimates by describing the probability of damage occurrence in a structure for post-earthquakes (HAZUS MH-MR5). This analysis can be conducted for buildings individually or for a stock of buildings. For instance, a study by Tatangelo et al (2024) demonstrates that typological fragility curves developed using macro-seismic data from 56,338 buildings affected by the 2009 L'Aquila earthquake provide significant insights into how different structural types behave under seismic loads, particularly when undamaged buildings are considered to reduce uncertainties at lower PGA levels. The inclusion of undamaged buildings has a substantial impact on the curves at low damage levels and low Peak Ground Acceleration (PGA) but becomes less relevant for higher PGAs.

Cimellaro et al. (2006) divided fragility curves into two parts: empirical and analytical fragility curves. Empirical fragility curves are derived from field data collected based on damages resulting from the past earthquakes. Conversely, analytical fragility curves can be generated using seismic response data obtained from ground motions while analyzing the structure. The fragility curve is graphical representation of earthquake intensity, measured in terms of spectral displacement (S_d), peak ground acceleration (PGA), and the probability of exceedance.

There are various methods to calculate the fragility curves of a structure, HAZUS MH MR4 (2003) proposed Eq. (2) for developing fragility curves.

$$P\left[\left(ds|S_d\right)\right] = \Phi\left[\frac{1}{\beta_{ds}}\ln\left(\frac{S_d}{\overline{S}_{d,}ds}\right)\right] \tag{2}$$

where *ds* describes the damage state level of a building which can be slight (*ds1*), moderate (*ds2*), extensive (*ds3*), and complete (*ds4*) damage state. S_d is the spectral displacement. $\overline{S}_{d,}ds$ is the median value of the spectral displacement for related damage level (*ds1, ds2, ds3, ds4*). β_{ds} is the standard deviation of the natural logarithm of the damage state (*ds*) and Φ is the standard normal cumulative distribution function.

Every damage level is described by ($\overline{S}_{d,}ds$) and (β_{ds}), which have different values for each damage level. The (β_{ds}) values can be directly extracted from tables or formulas provided by HAZUS MH-MR5 (2003). ($\overline{S}_{d,}ds$) values can be obtained through various

formulas (Giovinazzi 2005; Barbat et al. 2006; Kappos et al. 2006) and will be discussed in detail.

Furthermore, a MATLAB-coded software developed by Baltzopoulos et al. (2017), named SPO2FRAG, is designed for deriving fragility curves using pushover analysis results.

2.2.2 Vulnerability analysis

The vulnerability curve, a cumulative combination of discrete damage probabilities and mean damage factors (MDFs), shows the damage probability of a structure. Hence, fragility analysis is a prerequisite for the determination of the vulnerability curves.

These curves are obtained by Eq. (3) (Sadeghi et al. 2015):

$$\text{Vulnerability } (\%) = \sum_{ds=1}^{N} \{P[ds = DS] \times MDF_{ds}\} \tag{3}$$

where (ds) is the damage state, $P[ds = DS]$ is the discrete probability of the damage state and (MDF_{ds}) is the mean damage factor of a specific damage state (slight, moderate, extensive, collapse).

The MDFs values can be obtained from sources such as HAZUS MH MR4 (2003), FEMA-356, ATC-13 and EMS-98. In this study, the methodology presented in HAZUS MH MR4 (2003) is employed for the determination of the fragility curves. Thus, the MDFs values prepared by HAZUS MH MR4 (2003) (Table 1) are utilized in this study.

As indicated in Table 1, MDF represents the average value of the damage factor range.

The discrete damage probabilities are obtained using Eq. (4) (HAZUS MH MR4, 2003):

$$\begin{aligned} P\left[ds = complete\right] &= P\left[ds \geq complete\right] \\ P\left[ds = extensive\right] &= P\left[ds \geq extensive\right] - P\left[ds \geq complete\right] \\ P\left[ds = moderate\right] &= P\left[ds \geq moderate\right] - P\left[ds \geq extensive\right] \\ P\left[ds = slight\right] &= P\left[ds \geq slight\right] - P\left[ds \geq moderate\right] \end{aligned} \tag{4}$$

Finally, the vulnerability curve can be generated using Eq. (3).

2.3 Seismic resilience

The final step of the methodology is the determination of the loss functionality and the seismic resilience of the structure. As illustrated in Fig. 1, a resilience curve can be divided into three parts. The structure shows 100% functionality until t1; thereafter, at t1, when an event occurs, a sudden drop in the curve is observed, and referred to as functionality loss.

Table 1 Mean damage factors as per HAZUS MH MR4 (2003)

Damage state	Damage factor range (%)	Mean damage factor (%)
Slight	> 0–4	2
Moderate	4–16	10
Extensive	16–84	50
Collapse (complete)	100	100

The second part of the curve, which can withstand the event, is called robustness. It represents the strongest part of the structure that can maintain functionality against the natural hazard event. The third part of the curve is the recovery function, which can take on linear, exponential, or trigonometric (Fig. 6). The recovery curve is the function of event time. Consequently, an increase in recovery time (T_{RE}) causes a decrease in rapidity and vice versa.

2.3.1 The Functionality of a structure

As aforementioned, when a structure is exposed to a hazard event, it loses its functionality. The functionality of a structure can be determined using Eq. (5) (Cimellaro et al. 2010b):

$$Q(t) = 1 - L\left(I, T_{RE}\right)\left[H\left(t - t_{0E}\right) - H\left(t - \left(t_{0E} + T_{RE}\right)\right)\right] f_{rec}\left(t, t_{0E}, T_{RE}\right) \quad (5)$$

where Q(t) is the functionality of a structure, $L\left(I, T_{RE}\right)$ is the loss functionality, $H\left(t - t_{0E}\right)$ is the Heaviside function.

As indicated by Eq. (5), the functionality function is a combination of loss function, Heaviside function, and recovery function.

Various formulas can be employed to derive functionality loss that relies on both intensity and recovery time (e.g., Samadian et al. 2019). This will be explained in detail in the following pages.

The Heaviside function is consistently either zero or one, contingent upon the sign of a number. For positive numbers, it assumes a value of one, while for negative numbers, it adopts a value of zero. In brief, it can be written as H (positive number or zero) = 1, H (negative number) = 0.

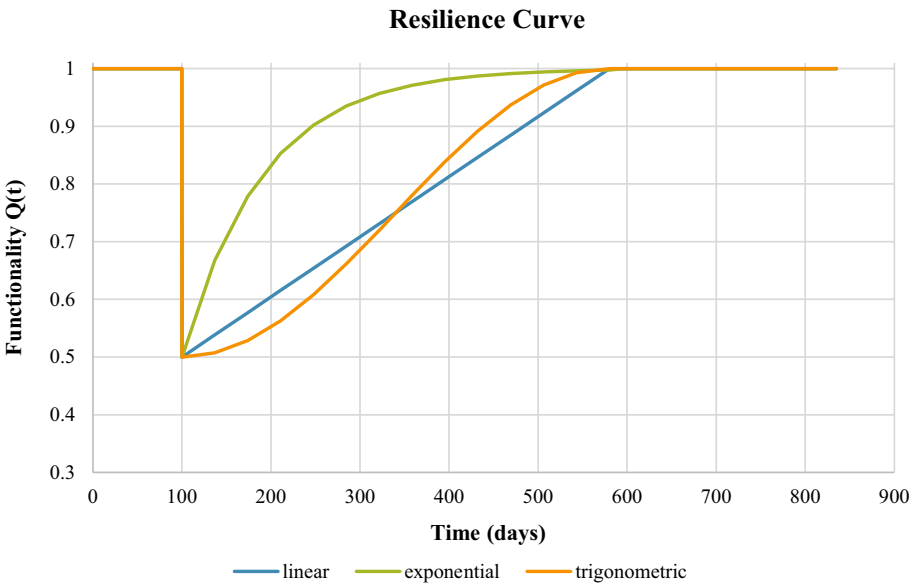

Fig. 6 Types of recovery curves

The recovery function comprises three categories, each acquired through a specific equation. The equations are presented below. (Cimellaro et al., 2005):

In the case of linear recovery function:

$$f_{rec}\left(t, T_{RE}\right) = \left(1 - \frac{t - t_{0E}}{T_{RE}}\right) \tag{6}$$

In the case of exponential recovery function:

$$f_{rec}(t) = \exp\left[-\left(t - t_{0E}\right)\left(\frac{\text{Ln}\,(200)}{T_{RE}}\right)\right] \tag{7}$$

In the case of trigonometric recovery function:

$$f_{rec}(t) = 0.5\left\{1 + \cos\left[\frac{\pi\left(t - t_{0E}\right)}{T_{RE}}\right]\right\} \tag{8}$$

Linear recovery function is the simplest form and is used where there is a lack of details about readiness, accessibility to the sources, and social reaction. Conversely, the exponential recovery function is employed when the primary social facilities are available, as depicted by its curve in Fig. 6. The rapidity on the first days is at a high level; however, as it approaches the end, the rapidity diminishes more gradually. The trigonometric recovery function is applied in situations where there is ais an inadequacy of resources or organizations. The rapidity can be either decreased or increased during the repairing procedure (Cimellaro et al. 2010b).

The event time (t_{0E}) refers to the period when the event occurs, and it is the time when the structure starts losing its functionality. T_{RE} constitutes the recovery time in which the structure will be repaired to recover its functionality to its previous form. It is one of the critical issues and can be problematic to choose the correct and exact recovery time. Generally, it is shorter than the control time, and the dimension relies on the seismic intensity, accessibility to resources materials and employers (Cimellaro et al. 2010b). The control time (T_{LC}) represents the economic life of a structure, commonly established 50 years for reinforced concrete structures.

2.3.2 Functionality loss

An earthquake can cause structural and non-structural damage. These damages can affect the functionality of a structure, particularly structural damages which are directly linked to the functionality loss of a structure. Seismic losses in a structure can be separated into two parts: the direct losses (LD) and the indirect losses (LI). The direct losses encompass economy and casualties, while the indirect losses also has two aspects: indirect economic losses and indirect casualties (Cimellaro et al. 2010b).

Various formulas can be employed to obtain loss functionality. Cimellaro et al. (2010b) suggested Eq. (9):

$$L_{DE}(I) = \sum_{J=1}^{N}\left[\frac{C_{S,J}}{I_S}\cdot\prod_{i=1}^{T_i}\frac{\left(1+\delta_i\right)}{\left(1+r_i\right)}\right]\cdot P_J\{\cup_{i=1}^{n}(R_I \geq r_{\lim i})/I\} \tag{9}$$

where (δ_i) and (r_i) are the annual depreciation and discount rates, respectively. These two parameters may vary from country to country and even from time to time. For instance, the depreciation rate is %2 for reinforced concrete buildings in Turkey. (P_j) is the probability of exceedance; (T_i) is the time range between the first investment and occurrence of an extreme event; $(C_{S,J})$ and (I_S) are the repairing and replacement costs of the damaged structure, respectively.

Furthermore, Samadian et al. (2019) proposed Eq. (10):

$$L_{DE}(I) = \frac{1}{K} \cdot \sum_{J=1}^{N} \left[\frac{C_{S,J}}{I_S} \cdot \prod_{i=1}^{T_i} \frac{(1+\delta_i)}{(1+r_i)}\right] \cdot \text{ Damage (\%)} \tag{10}$$

where (K) is the awareness factor indicates the quantity of information about construction quality and takes a value of 1for structures with complete awareness and 0.75 for all other cases. Damage (%) value will be based on vulnerability curves.

3 Case study: seismic resilience of a school building in Mugla

3.1 Structural model

Milas, situated in Mugla, is located at coordinates 37.3116° N, 27.7808° E. This case study focuses on a school building, comprising a basement and three normal floors, in a 576 m^2 area. Properties and the dimensions of the building are listed in Table 2. The distance between the axes along the building's longer side measures 4.00 m, with exceptions for the initial bay at 4.05 m and the final bay at 3.85 m. The spacing between the axes along the short side of the building are 3.85 m, 4.00 m, 4.00 m, and 3.85 m. The basement floor of the building is encompassed by shear walls, as depicted in the 3D view of the structure (Fig. 7). Furthermore, each floor features stair shear walls. The shear wall which connects beams, columns and floors is located across the height of the building positioned centrally along the x-axis but is off-center along the y-axis. The wall which has a height of 11.3 (m) and a width of 4 (m) is designed as a slender wall that is prone to flexural behavior under lateral loads. Special attention is given to the vertical and horizontal reinforcements

Table 2 General properties of the structure

Part of structure	
Basement story height (m)	2.9
Normal story height (m)	2.8
Beam (cm)	30×40
Foundation columns (cm)	40×40
Normal floor columns (cm)	35×35
Slab thickness (cm)	15
Shear wall thickness (cm)	25
Building width (m)	16
Building length (m)	36
ρ (Column)	1.51%
ρ (Beam)	0.88%
ρ (Shear Wall)	0.58%

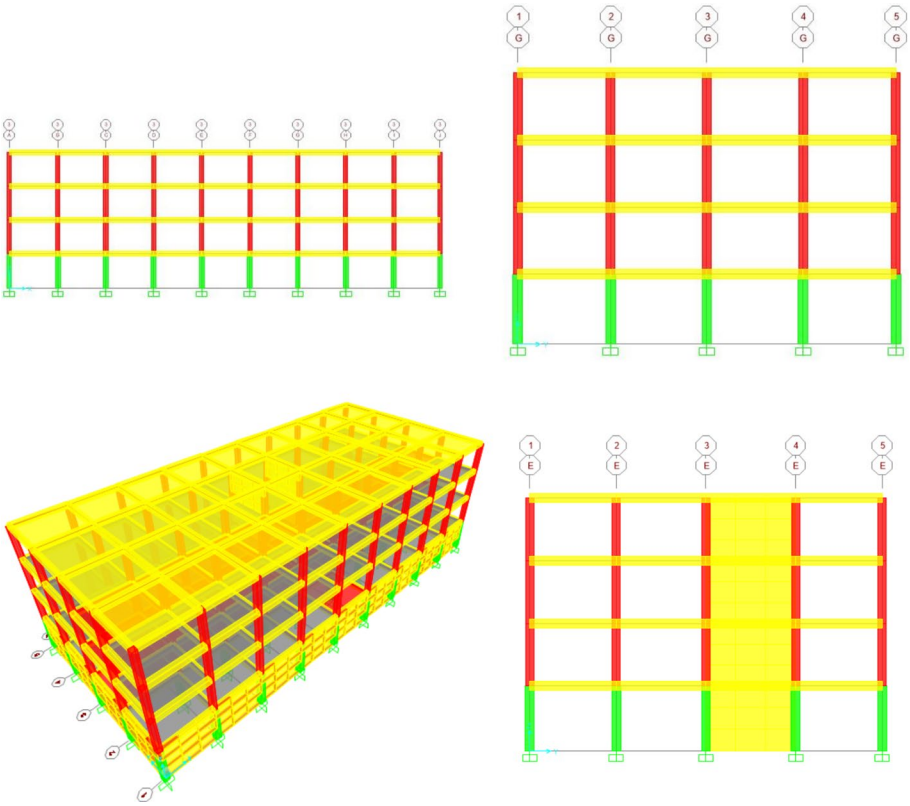

Fig. 7 Model of the school building in SAP 2000 software

to resist the resulting moments, and to prevent buckling under the axial forces especially at the critical zone near the base of the wall. C30 and S420 are the materials for concrete and steel, respectively.

Soil class is a crucial parameter in defining the response spectrum parameters such as S_{DS} and S_{D1}. Based on the geotechnical report, the soil class is ZB. Soil class ZB is a group of soil that has slightly weathered, medium-tough rocks and has V_{S30} of (760–1500) m/s based on the Turkish Building Earthquake Code (2018). For this school area, the PGA is 0.38 g, SDS and SD1 values are 0.799 and 0.166, respectively.

As mentioned earlier and shown in 3D-view of the structure (Fig. 7), the basement floor of the building has shear walls, and the structure exhibits a very slight irregularity in only to one direction (y-direction), This is due to the shear walls of the stairs, resulting in a minor small eccentricity in y-direction.

S420 rebars are used for both beams and columns. For the basement and normal story columns, 12Ø16 and 12Ø14 rebars are used, respectively. The columns are reinforced with Ø8/10 stirrups in the confinement areas and Ø8/15 stirrups in the middle sections, providing adequate shear resistance. For beam sections, 4Ø14 rebars are placed at the bottom and 2Ø14 rebars are placed at the top of the section. Additionally, Ø8/10 and Ø8/20 stirrups are used in the confinement and middle areas of the beams, accordingly. For the shear walls, Ø16/150 and Ø14/200 vertical reinforcements are used in the boundary zones and web

region, respectively. Ø10/150 reinforcements are placed horizontally in both the web and boundary zones of the wall. Additionally, the Ø8/150 stirrups are used in the boundary zones.

3.2 Structural modelling

The structural software SAP2000 is used for the modeling of the structure. Figure 7 depicts the undeformed shape of the modeled building, and details of the first five potential deformed mode shapes due to the earthquake are listed in Table 3.

The first mode represents the deformation in x-direction. The second mode involves torsional deformation in z-direction, leading to displacements in both (x) and (y) directions. The third possible deformation is the displacement of the structure along the y-direction.

3.3 Pushover analysis

Nonlinear static pushover analysis is widely employed method for the seismic analysis of buildings. To conduct the pushover analysis, it is necessary to obtain seismic loads affecting the building. The total self-weight of the structure is calculated. The seismic loads are applied to the center of the structure (mass center) in x-direction with both positive and negative moments. Similarly, the seismic loads are applied to the structure in y-direction with both clockwise and counterclockwise moments.

A nonlinear static pushover analysis is performed under (P-Δ) effects with assigned plastic hinges as mentioned in Sect. 2.1.2.

M3 plastic hinges, which represent moment-rotation relationships, flexural behaviour and inelastic deformations, are assigned to the ends of beams. For columns, P-M2-M3 hinges are assigned, representing axial force–deformation and moment-rotation relationships, as well as flexural behaviour. The P hinges account for axial deformations, while the M2 and M3 hinges capture various aspects of the column's flexural response, including inelastic behaviour and potential failure modes.

3.4 Building response

The structure is performed for both (x) and (y) directions. The capacity curves are obtained as shown in Fig. 8. The capacity curve in the y-direction direction exhibits more elasticity properties, whereas the capacity curve in the x-direction is turned into a plastic stage. The main reason for this is the orientation of the shear wall along the y-direction that provides significant lateral stiffness and strength to the structure. Therefore, the critical condition of

Table 3 Periods and frequencies of the structure for each mode

Model No	Period (s)	Frequency (Hz)
1	0.62	1.61
2	0.57	1.75
3	0.36	2.77
4	0.2	4.99
5	0.18	5.57

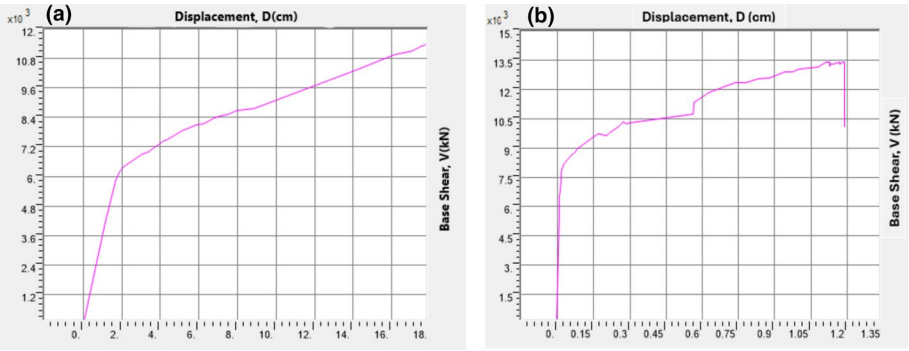

Fig. 8 Capacity curves in: **a** x-direction and **b** y-direction

the structure exhibits in the x-direction is considered. The forthcoming procedure in the study is based on the results obtained from the pushover analysis in the x-direction.

The aforementioned capacity curve in the x-direction is converted into the acceleration displacement response spectrum (Fig. 9). Afterward the median spectral displacement values are used to get the fragility curves discussed in the following sections.

3.5 Fragility analysis

Fragility curves of the structure are derived from Eq. (2), as mentioned and explained in the preceding pages. Initially, it is required to acquire the ($\overline{S}_{d,}$ds) and (β_{ds}) values. (β_{ds}) takes different values at each damage state and can be directly retrieved from HAZUS MH-MR-5 (2003), relying on the building types elucidated by HAZUS MH-MR-4 (2003) and degradation factors (kappa factor, k). In accordance with the building types specified in HAZUS MH-MR-4 (2003), the structure associated with reinforced concrete low-rise building groups (C1L). Likewise, ($\overline{S}_{d,}$ds) changes for each damage state.

In this study, degradation factors are chosen based on the damage states. Minor degradation (k = 0.9) for slight damage state, major degradation (k = 0.5) for moderate damage

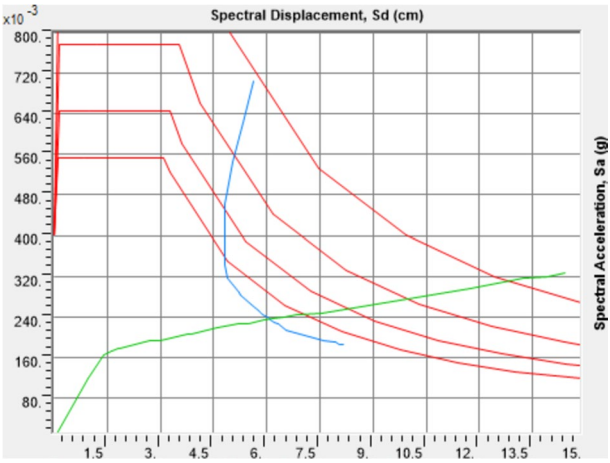

Fig. 9 Acceleration displacement spectrum. The curve in red color is called as the demand spectrum. The curve in blue color is the demand curve, and the curve in green color is the capacity curve. The intersection point of the demand curve and the capacity curve is called as the performance point (Alashker et al. 2015). The performance points for (V, D) and (Sa, Sd) are obtained. It is based on ATC-40

Table 4 (β_{ds}) values (HAZUS MH-MR-5, 2003)

Damage state (ds)	(β_{ds})
Slight	0.7
Moderate	0.85
Extreme	0.95
Collapse	0.95

Table 5 $\left(\overline{S}_{d,}ds\right)$ values based on Giovinazzi (2005), Barbat et al. (2006) and Kappos et al. (2006)

Models	Models for Median spectral displacement values ($\overline{S}_{d,}ds$)			
	Slight	Moderate	Extreme	Collapse
Giovinazzi (2005)	$0.7S_{dy}$	$1.5S_{dy}$	$0.5(S_{du}+S_{dy})$	S_{du}
Barbat et al. (2006)	$0.7S_{dy}$	S_{dy}	$S_{dy}+0.25(S_{du}-S_{dy})$	S_{du}
Kappos et al. (2006)	$0.7S_{dy}$	S_{dy}	$2S_{dy}$	S_{du}

state, extreme degradation (k = 0.1) for extreme and collapse damage states are considered (HAZUS MH-MR-4, 2003). The related (β_{ds}) values are outlined in Table 4.

$\left(\overline{S}_{d,}ds\right)$ is a function of the yield displacement (S_{dy}) and the ultimate displacement (S_{du}). Researchers have been endeavoring to present appropriate models for obtaining median values of the spectral displacements. In this research, $\left(\overline{S}_{d,}ds\right)$ values are derived by using three models proposed by Giovinazzi (2005), Barbat et al. (2006) and Kappos et al. (2006). These models were selected to provide more comprehensive and accurate risk assessment. The equations for deriving $\left(\overline{S}_{d,}ds\right)$ values based on these models are listed in Table 5.

The yield and ultimate spectral displacement values are predicted from the capacity curve, and the median spectral displacements are then obtained using the formula from the models. The median spectral displacement values depend on both the yield and ultimate spectral displacement values. According to these three models, the spectral displacement value for the slight damage level (Sd) is considered to be 70% of the yield point, while for the collapse damage level (Sd), it is assumed to be at the ultimate capacity point of the curve. In this study, a single capacity curve is used, leading to one yield capacity point and an ultimate capacity point for all three models. As a result, the spectral displacement values for slight and collapse damage levels have similar for all three models, as they depend only on the yield and ultimate capacity point of the curve.

As outlined in Table 5, all models have the same $\overline{S}_{d,}ds$ values for slight and collapse damage states. However, for moderate and extreme damage states each model has different $\overline{S}_{d,}ds$ values. The calculated $\overline{S}_{d,}ds$ values for the case study are listed in Table 6.

The fragility curves derived from the mentioned $\overline{S}_{d,}ds$ values (Table 6) are depicted in Fig. 10.

It can be seen from the illustrated fragility curves (Fig. 10) that the probability of slight and collapse damage levels is the same for all three types of fragility curves. However, there is an increase in damage probability in moderate and extreme damage levels. Especially, the fragility curves based on Kappos et al. (2006) model has a significant increase in

Table 6 Median spectral displacement values $\left(\overline{S}_{d,}ds\right)$ for the building

Models	Median spectral displacement values $\left(\overline{S}_{d,}ds\right)$)			
	Slight (cm)	Moderate (cm)	Extreme (cm)	Collapse (cm)
Giovinazzi (2005)	1.18	2.53	7.30	12.91
Barbat et al. (2006)	1.18	1.68	4.49	12.91
Kappos et al. 2006)	1.18	1.68	3.38	12.91

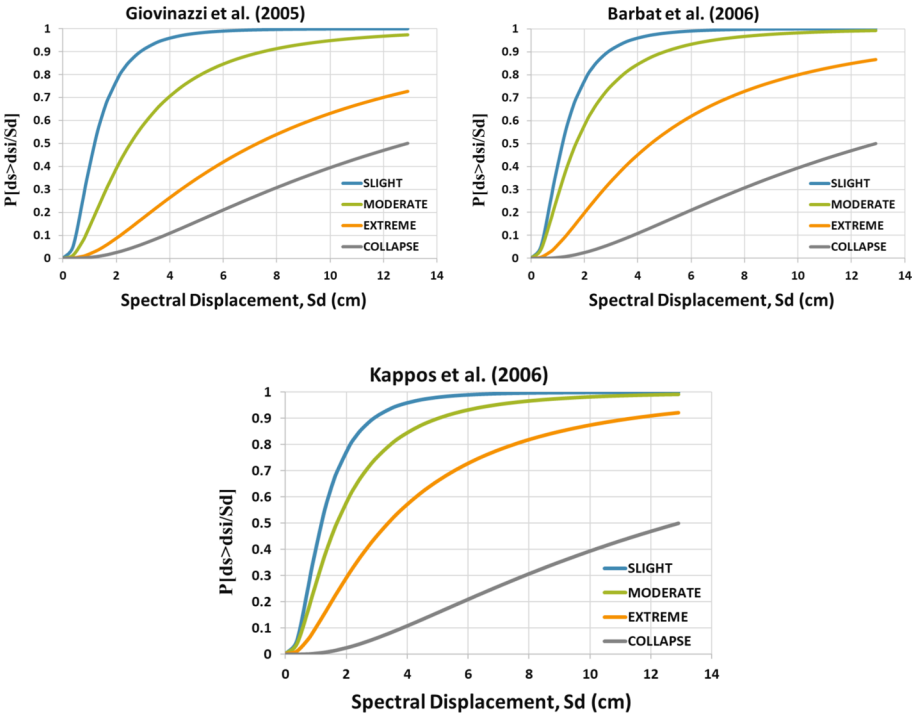

Fig. 10 Fragility curves based on Giovinazzi (2005), Barbat et al. (2006) and Kappos et al. (2006)

damage probability during the extreme damage level (Fig. 10). A summary of the damage probabilities occurring at maximum displacement is provided in Table 7.

3.6 Seismic loss

Vulnerability curves can be obtained directly from the fragility curves by using Eq. (3) and values listed in Table 1, which involves the mean damage factor (MDF) values. Since the fragility curves are generated for three different conditions according to the proposed models, there are correspondingly three different vulnerability curves identified. Figure 10

Table 7 Maximum damage probability of each model

Damage state	Maximum Damage probability (%)		
	Giovinazzi (2005)	Barbat et al. (2006)	Kappos et al. (2006)
Slight	99.9	99.9	99.9
Moderate	97.23	99.167	99.167
Extreme	72.6	86.67	92.11
Collapse	50	50	50

Table 8 Potential maximum damage (%)

Damage (%)		
Giovinazzi (2005)	Barbat et al. (2006)	Kappos et al. (2006)
63.8	69.6	71.77

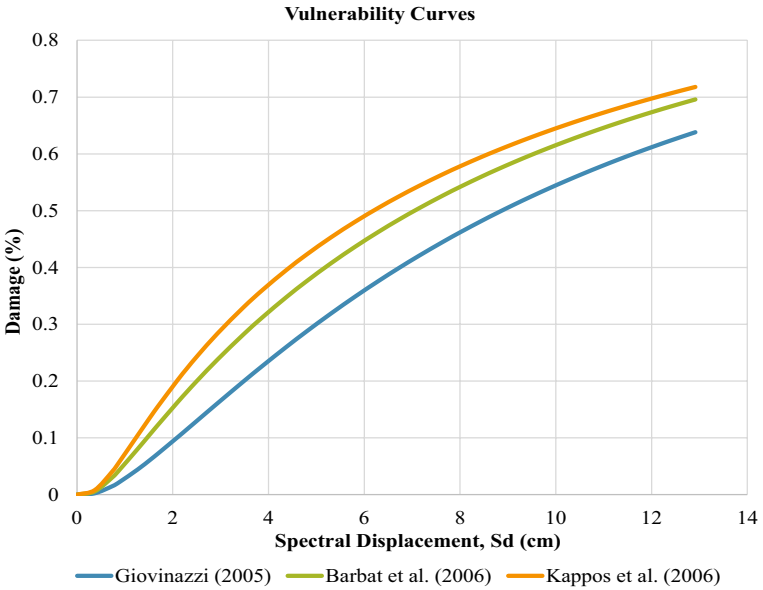

Fig. 11 Comparison of the results along with the vulnerability curves

displays the vulnerability curve derived from the prepared fragility curves, as illustrated in the preceding pages. The maximum damage (%) of the structure is detailed in Table 8.

As illustrated in Fig. 11, each vulnerability curve has a different damage level. The lowest damage (%) is derived from the vulnerability curve based on Giovinazzi (2005). In the contrast, the highest damage (%) is obtained from the vulnerability curve based

on Kappos et al. (2006). Therefore, it is a critical condition for the building. The resilience procedure will proceed based on the vulnerability curve.

3.7 Seismic Resilience of the structure

The final part of the study involves the analysis of resilience. It is derived from Eq. (5), which integrates three equations: loss function, recovery function and Heaviside function. In this case study, the resilience curve is obtained by exclusively considering the structural damages (direct damages) occurred in the structure as a result of seismic activity. As mentioned earlier, the recovery function has three types. The resilience curve will be acquired based on each individual function. Therefore, we will have three different resilience curves. The important parameters of the recovery function are event and recovery times. Selecting the recovery time is one of the complex issues. Generally, the schools in Turkey are reconstructed in 6–10 months. Therefore, the recovery time is assumed to be a value of 300 days for the purpose of this study.

To get the loss functionality of the structure, it is necessary to understand the damage (%), depreciation and annual discount rates, and $\left(\frac{C_{S,J}}{I_S}\right)$ ratio. The damage (%) is extracted directly from the vulnerability curves. The maximum damage is obtained (72%) as a result of these vulnerability curves. In this analysis, depreciation and annual discount rates are assumed to be 2% and 10%, respectively. the ratio is one of the important parts of the loss functionality which has significant effects on the functionality value. An increase in the $\left(\frac{C_{S,J}}{I_S}\right)$ ratio causes a decrease in the functionality of the structure (functionality loss increases). In this case study, three different $\left(\frac{C_{S,J}}{I_S}\right)$ ratios (0.25, 0.35, 0.45) are assumed. Subsequently, applying Eq. (10), the loss functionality is derived and corresponding resilience curves are plotted for each $\left(\frac{C_{S,J}}{I_S}\right)$ ratio, as depicted in Fig. 12.

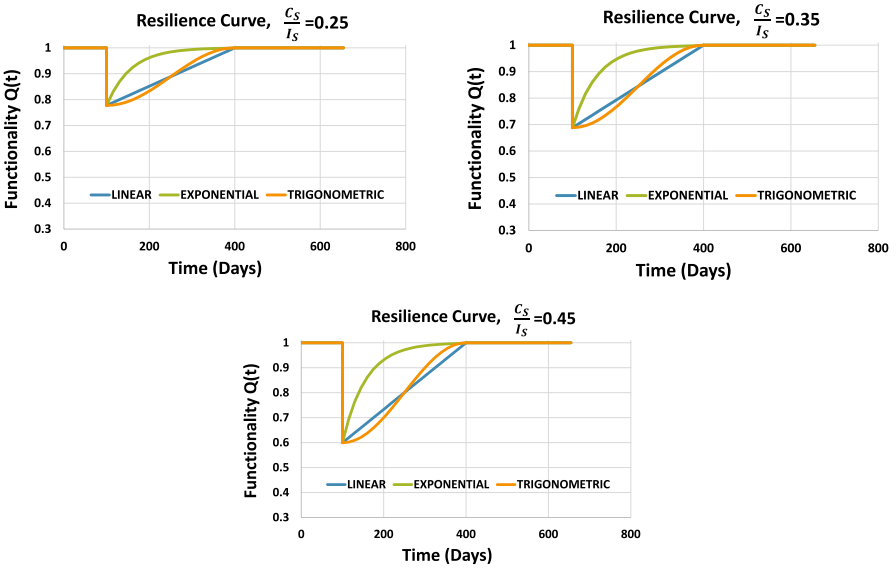

Fig. 12 Resilience curve of the building with different $\left(\frac{C_{S,J}}{I_S}\right)$ values

As illustrated in Fig. 12, it can be seen clearly that there is a significant difference in loss functionality. The loss functionality increases from 22 to 40%.

4 Conclusions

In this research, damage assessment (fragility curves, vulnerability curves) and resilience of an RC school building are presented applying nonlinear static pushover analysis and the HAZUS MH MR4 (2003) methodology. Three different methods based on Giovinazzi (2005), Barbat et al. (2006) and Kappos et al. (2006) to compare the median spectral displacement $\left(\overline{S}_{d,}ds\right)$ values for fragility curves are utilized. The $\left(\overline{S}_{d,}ds\right)$ values acquired for both slight and collapse damage states consistent across all three models. Thus, there is no distinction in the damage probabilities of these two damage states either. Nevertheless, there is a discrepancy in the values obtained for both moderate and extreme damage states. Therefore, all three models give three different damage probabilities for moderate and extreme damage states. The fragility curves generated through the application of the Kappos et al. (2006) model exhibit the highest damage probabilities compared to the other two models. As a result, the vulnerability curve derived from Kappos et al. (2006) has the highest damage (%) attributed to the seismic resilience curve. In addition, the study concluded that $\left(\frac{C_{S,J}}{I_S}\right)$ ratio and recovery time (T_{RE}) have significant effects on the rapidity of reconstruction or repairing of the structure. Despite that, the $\left(\frac{C_{S,J}}{I_S}\right)$ also influences the loss of functionality of the structure. It is evident that, an increase in the $\left(\frac{C_{S,J}}{I_S}\right)$ ratio causes an increase in the loss of functionality. All in all, the important factors influencing the resilience curve are $\left(\frac{C_{S,J}}{I_S}\right)$ ratio, $\left(\overline{S}_{d,}ds\right)$ values, recovery time, and either seismic damage (%) or vulnerability curve. These factors collectively contribute to determining the characteristics of the resilience curve. Consequently, this research study highlights a detailed comparison of three established methodologies (Giovinazzi 2005; Barbat et al. 2006; Kappos et al. 2006) for deriving median spectral displacement values and fragility curves to perform damage assessment of the school building and subsequently obtain its seismic resilience curve. The study shows how different models impact the fragility and vulnerability curves, particularly at moderate and extreme damage states. It will form a basis for the resilience analysis of school buildings in this context, demonstrating how traditional school buildings respond to seismic events. The outcomes provide practical guidance for engineers and policymakers, contributing to the development of more resilient educational infrastructures in seismic-prone regions. Certainly, if we elaborate on this; the research holds significance in revealing the effect of the models intended for use in the regional or building-based resilience analysis. In some regions, schools are generally of the same characteristics. When calculating the resilience for any given school, the effect of fragility curves used for this type of structure on the resilience will provide guidance.

Author Contributions All authors contributed to the study. All authors read and approved the final manuscript.

Funding The authors declare that no funds, grants, or other support were received during the preparation of this manuscript.

Declarations

Competing Interests The authors have no relevant financial or non-financial interests to disclose.

References

Alashker Y, Nazar S, Ismaiel M (2015) Effects of Building Configuration on Seismic Performance of RC Buildings by Pushover Analysis. Open J Civ Eng 2:203–213. https://doi.org/10.4236/ojce.2015.52020

ATC-13 (1985) Earthquake damage evaluation data for California, CA: Applied Technology Council (ATC), Redwood City, USA. https://www.atcouncil.org/pdfs/atc13.pdf.

ATC-40 (1996) Seismic evaluation and retrofit of concrete buildings, CA: Applied Technology Council (ATC) Redwood City, USA.

Baltzopoulos G, Baraschino R, Iervolino I, Vamvatsikos D (2017) SPO2FRAG: Software for seismic fragility assessment based on static pushover. Bull Earthq Eng 15:4399–4425

Barbat AH, Pujades LG, Lantada N (2006) Performance of Buildings under Earthquakes in Barcelona. Spain Comput-Aided Civ Infrastruct Eng 8(21):573–593. https://doi.org/10.1111/j.1467-8667.2006.00450.x

Bruneau M, Chang SE, Eguchi RT, Lee GC, O'Rourke TD, Reinhorn AM, Shinozuka M, Tierney K, Wallace WA, Winterfeldt DV (2003) A framework to quantitatively assess and enhance the seismic resilience of communities. Earthq Spectra 19(4):733–752. https://doi.org/10.1193/1.1623497

Bruneau M, Reinhorn AM (2004) Seismic Resilience of Communities Conceptualization and Operationalization. Proc Int Workshop on Performance Based Seismic-Design, Bled-Slovenia, June.

Burton HV, Deierlein G, Lallemant D, Singh Y (2017) Measuring the Impact of Enhanced Building Performance on the Seismic Resilience of a Residential Community. Earthq Spectra 33(4):1347–1367https://doi.org/10.1193/040916eqs057m.

Cimellaro GP, Reinhorn AM, Bruneau M (2005) Seismic Resilience of a Health care facility. Proc of the 2005 ANCER Annu Meet, Session III, November 10–13, Jeju, Korea.

Cimellaro GP, Reinhorn AM, Bruneau M, Rutenberg A (2006) Multi-Dimensional Fragility of Structures:Formulation and Evaluation. Report number: MCEER-06–0002 Affiliation: University at Buffalo – SUNY. https://www.researchgate.net/publication/309791885.

Cimellaro GP, Reinhorn AM, Bruneau M (2010a) Seismic resilience of a hospital system. Struct Infrastruct Eng 6(1–2):127–144. https://doi.org/10.1080/15732470802663847

Cimellaro GP, Reinhorn AM, Bruneau M (2010b) Framework for analytical quantification of disaster Resilience. Eng Struct 32:3639–3649. https://doi.org/10.1016/j.engstruct.2010.08.008

EMS-98 (1998) European Macroseismic Scale. European Seismological Commission, sub commission on Engineering Seismology, Luxembourg.

FEMA-356 (2000) Prestandard and Commentary for the Seismic Rehabilitation of Buildings. American Society of Civil Engineers, Washington, USA

FEMA-P58 (2012) Next-Generation Methodology for Seismic Performance Assessment of Buildings. prepared by the Applied Technology Council for the Federal Emergency Management Agency, Report No. FEMA P-58, Washington, DC.

Freeman SA, Nicoletti JP and Tyrell JV (1975) Evaluations of Existing Buildings for Seismic Risk - A Case Study of Puget Sound Naval Shipyard, Bremerton, Washington., Proc U.S. National Conf Earthq Eng, Berkeley, USA, 113–122.

Giovinazzi S (2005) The Vulnerability Assessment and the Damage Scenario in Seismic Risk Analysis. Ph.D. Dissertation, Department of Civil Engineering, Technical University of Braunschweig.

González C, Niño M, Jaimes MA (2020) Event-based assessment of seismic resilience in Mexican school buildings. Bull Earthq Eng 18:6313–6336. https://doi.org/10.1007/s10518-020-00938-5

Hamadamin SS (2014) Pushover Analysis and Incremental Dynamic Analysis of Steel Braced Reinforced Concrete Frames. M.Sc Thesis, Department of Civil Engineering, Eastern Mediterranean University, Institute of Graduate Studies and Research, Famagusta, North Cyprus.

HAZUS MH-MR-4 Technical Manual (2003) Multi-hazard Loss Estimation Methodology. National Institute of Building Sciences, Washington DC, USA.

HAZUS MH-MR-5 Technical and User's Manual (2003) Earthquake loss estimation methodology. Department of Homeland Security and Federal Emergency Management Agency, Washington DC, USA.

Ince GÇ, Yılmazoğlu MU (2021) Probabilistic seismic hazard assessment of Muğla. Turkey Nat Hazards 107(2):1311–1340. https://doi.org/10.1007/s10518-006-9023-0

Kappos AJ, Panagopoulos G, Panagiotopoulos C, Penelis G (2006) A hybrid method for the vulnerability assessment of R/C and URM buildings. Bull Earthq Eng 4:391–413. https://doi.org/10.1007/s10518-006-9023-0

Motlagh ZS, Dehkordi MR, Eghbali M, Samadian D (2020) Evaluation of seismic resilience index for typical RC school buildings considering carbonate corrosion effects. Int J Disaster Risk Reduct 46:101511. https://doi.org/10.1016/j.ijdrr.2020.101511

Sadeghi M, Ashtiany MG, Lahiji NP (2015) Developing seismic vulnerability curves for typical Iranian buildings. Proc Inst Mech Eng o: J Risk Reliab 229(6):1–14. https://doi.org/10.1177/1748006X15596085

Samadian D, Ghafory-Ashtiany M, Naderpour H, Eghbali M (2019) Seismic resilience evaluation based on vulnerability curves for existing and retrofitted typical RC school buildings. Soil Dyn Earthq Eng 127:105844. https://doi.org/10.1016/j.soildyn.2019.105844

Sardari F, Dehkordi MR, Eghbali M, Samadian D (2020) Practical seismic retrofit strategy based on reliability and resiliency analysis for typical existing steel school buildings in Iran. Int J Disaster Risk Reduct 51:101890. https://doi.org/10.1016/j.ijdrr.2020.101890

Tatangelo M, Audisio L, D'Amato M, Gigliotti R (2024) Issues related to typological fragility curves derivation starting from observed seismic damage. Eng Struct 307:117853. https://doi.org/10.1016/j.engstruct.2024.117853.

Turkish Building Earthquake Code (2008) Disaster and Emergency Management Presidency (AFAD). Ankara, Turkey.

Xiong C, Huang J, Lu X (2019) Framework for city-scale building seismic resilience simulation and repair scheduling with labor constraints driven by time– history analysis. Comput-Aided Civ Infrastruct Eng 35(4):322–341. https://doi.org/10.1111/mice.12496

Yoon S, Joo Lee Y, Jo Jung H (2021) Flow based seismic resilience assessment of urban water transmission networks. Struct Eng Mech 79(4): 517–529. https://doi.org/10.12989/sem.2021.79.4.517.

Zhao T, Sun L (2021) Seismic resilience assessment of critical infrastructure-community systems considering looped interdependences. Int J Disaster Risk Reduct 59:102246. https://doi.org/10.1016/j.ijdrr.2021.102246